Iron−Sulfur Clusters with $SiMe_2$-Bridged Cyclopentadienyl Ligands: $[Me_2Si(\eta^5\text{-}C_5H_4)_2]_2Fe_5S_{12}$, $[Me_2Si(\eta^5\text{-}C_5H_4)_2]_2Fe_4S_6$, and $[Me_2Si(\eta^5\text{-}C_5H_4)_2]_2Fe_4S_6(CO)$†

Wouter van den Berg,‡ Lianne Boot,‡ Helma Joosen,‡ Johannes G. M. van der Linden,‡ Wil P. Bosman,‡ Jan M. M. Smits,‡ René de Gelder,‡ Paul T. Beurskens,‡ Jürgen Heck,*,§ and Anton W. Gal*,‡

Department of Inorganic Chemistry, Nijmegen SON Research Center, University of Nijmegen, Toernooiveld 1, 6525 ED Nijmegen, The Netherlands, and Institut für Anorganische und Angewandte Chemie, Universität Hamburg, Martin-Luther-King-Platz 6, 20146 Hamburg, Germany

Received July 26, 1996⊗

The synthesis and characterization of iron−sulfur clusters stabilized by dimethylsilyl-bridged cyclopentadienyl groups are reported. The thermal reaction of $Me_2Si(\eta^5\text{-}C_5H_4)_2Fe_2(CO)_4$ (**1**) with S_8 yields the tetranuclear cubane-type cluster compound $[Me_2Si(\eta^5\text{-}C_5H_4)_2]_2Fe_4S_6$ (**4**) and the pentanuclear cluster compound $[Me_2Si(\eta^5\text{-}C_5H_4)_2]_2Fe_5S_{12}$ (**3**) in high yields. The photochemical reaction of **1** with S_8 yields the tetranuclear cluster compound $[Me_2Si(\eta^5\text{-}C_5H_4)_2]_2Fe_4S_6(CO)$ (**5**), which contains one residual terminal carbonyl. The crystal structures of **3** and **4** have been determined. Crystal data: **3**·CH_2Cl_2, monoclinic, *C*2/*c*, $a = 23.480(13)$ Å, $b = 11.192$ (4) Å, $c = 17.84$ (3) Å, $\beta = 118.58(9)°$, $V = 4118(7)$ Å^3, $Z = 4$, $R = 0.078$; **4**, triclinic, $P\bar{1}$, $a = 8.4787(7)$ Å, $b = 12.9648$-(9) Å, $c = 13.4990(9)$ Å, $\alpha = 79.857(8)°$, $\beta = 75.293(8)°$, $\gamma = 74.041(11)°$, $V = 1370.9(2)$ Å^3, $Z = 2$, $R = 0.0447$. The Fe_5S_{12} core of **3** has a bowtie structure in which a central iron atom is octahedrally coordinated by six sulfur atoms from one tetrasulfido and four disulfido groups. The structure of **4** resembles the structure of the known iron−sulfur cluster $Cp_4Fe_4S_6$. However, **4** shows a markedly enhanced thermal stability compared to $Cp_4Fe_4S_6$. In their cyclic voltammograms, **4** and **5** exhibit electrochemical behavior typical of cubane-type Cp−iron−sulfur clusters, whereas the cyclic voltammogram of **3** is quite different. The ν_{CO} mode of **5** has been measured for four different oxidation states of the cluster by means of IR spectroelectrochemical methods. The Mössbauer spectra of **3** and $\mathbf{3}^+$ are in accordance with their pentanuclear structure.

Introduction

Dicyclopentadienyl ligands, $C_5H_4-X-C_5H_4$, e.g. with $X = SiMe_2$, impose geometrical constraints on dinuclear metal complexes. As a result, substantial changes in structures and properties can occur for these complexes when compared to their counterparts with nonbridged cyclopentadienyl groups.[1] In our studies on cubane-like tetrairon−sulfur cluster compounds $Cp_4Fe_4S_x$ ($x = 4-6$), the use of the dicyclopentadienyl ligand $C_5H_4-SiMe_2-C_5H_4$ instead of isolated cyclopentadienyl (Cp) ligands resulted in the hitherto unknown Fe_5S_{12} cluster compound $\{[Me_2Si(\eta^5\text{-}C_5H_4)_2]_2Fe_5S_{12}\}\{FeCl_4\}$, for which we recently reported the crystal and molecular structure.[2] This compound formed during prolonged (8 weeks) crystallization from dichloromethane/hexane of a reaction product that was unknown at that time. The initial reaction product apparently decomposes oxidatively to the monocationic Fe_5S_{12} cluster compound and $FeCl_4^-$.

In this paper, we show that the neutral cluster compound $[Me_2Si(\eta^5\text{-}C_5H_4)_2]_2Fe_5S_{12}$ (**3**) is a product from the thermal reaction of $Me_2Si(\eta^5\text{-}C_5H_4)_2Fe_2(CO)_4$ (**1**) with elemental sulfur. In this reaction, $[Me_2Si(\eta^5\text{-}C_5H_4)_2]_2Fe_4S_6$ (**4**) is also formed. The photochemical reaction of **1** with elemental sulfur generates the Fe_4S_6 cluster compound $[Me_2Si(\eta^5\text{-}C_5H_4)_2]_2Fe_4S_6(CO)$ (**5**), in which one terminal CO ligand is still present.

Experimental Section

General Methods. All manipulations were carried out under a purified N_2 atmosphere, using standard Schlenk techniques, unless indicated otherwise. Al_2O_3 (aluminum oxide 90, neutral, activity III, Merck) was heated at 200 °C under 10^{-3} mbar pressure for 3 days and subsequently deactivated with 5% (w/w) H_2O saturated with N_2. SiO_2 (100, Merck) was evacuated under 10^{-3} mbar pressure for 3 days. $Fe(CO)_5$ was filtered and bubbled with N_2 prior to use. The solvents were dried and subsequently distilled under N_2 atmosphere according to standard literature procedures.[3]

Tetrabutylammonium hexafluorophosphate (TBAH, Fluka) and $P(C_6H_5)_3$ (Merck) were used as received. S_8 (Interpharm) was sublimed under reduced pressure. $[Fc]PF_6$[4] and $Me_2Si(C_5H_5)_2$[5] were prepared by published procedures.

Physical Measurements. FAB mass spectra were recorded on a VG 7070 mass spectrometer. FD mass spectra were recorded on a JEOL JMS-SX/SX102A at the University of Amsterdam, The Netherlands. ^{1}H and ^{13}C NMR and ^{1}H 2D COSY NMR spectra were recorded on a Bruker AC 100 MHz FT spectrometer, a Bruker WM 200 FT spectrometer, a Varian Gemini 200 BB spectrometer, and a Bruker AM 500 MHz FT spectrometer. Mössbauer spectra were recorded by Dr. Mulder at the Kamerlingh Onnes Institute of the University of Leiden, The Netherlands, using a constant-acceleration spectrometer equipped with a ^{57}Co source in a Rh matrix (**3**, **3**(PF_6)) and by Dipl. Chem. S. Bieber at the University of Hamburg, Germany, using a conventional ^{57}Fe Mössbauer equipment (**4**, [**4**]PF_6). Powder samples were either dispersed in boron nitride (**3**, [**3**]PF_6), sealed in

† Cooperative Effects in π-Ligand-Bridged Dinuclear Complexes. 18. Dedicated to Prof. Dr. M. Herberhold on the occasion of his 60th birthday.

‡ University of Nijmegen.

§ Universität Hamburg.

⊗ Abstract published in *Advance ACS Abstracts,* March 15, 1997.

(1) Abriel, W.; Baum, G.; Heck, J.; Kriebisch, K.-A. *Chem. Ber.* **1990**, *123*, 1767−1778.

(2) Van den Berg, W.; Boot, C. E.; Van der Linden, J. G. M.; Bosman, W. P.; Smits, J. M. M.; Beurskens, P. T.; Heck, J. *Inorg. Chim. Acta* **1994**, *216*, 1−3.

(3) Perrin, D. D.; Armarego, W. L. F.; Perrin, D. R. *Purification of Laboratory Chemicals*; Pergamon Press: Oxford, U.K., 1966.

(4) Gill, N. S.; Taylor, F. B. *Inorg. Synth.* **1967**, *9*, 136−142.

(5) Yasuda, H.; Nagasuna, K.; Akita, M.; Lee, K.; Nakamura, A. *Organometallics* **1984**, *3*, 1470−1478.

S0020-1669(96)00900-7 CCC: $14.00

brass rings with Kapton windows, and studied at 77 K or used neat (**4**, [**4**]PF_6), transferred to a small Schlenk flask with Mylar foil windows, and studied at room temperature. Isomer shifts are reported relative to Fe metal at 298 K in both cases. IR spectra were recorded on a Perkin-Elmer 1720-X FTIR spectrometer. EPR spectra were recorded on a Bruker ESP 300 spectrometer and a Bruker ER-220D-LR spectrometer. Cyclic voltammetry and differential-pulse voltammetry measurements were performed using an EG&G Princeton Applied Research Model 273 galvanostat/potentiostat. A conventional three-electrode cell, with Pt working and auxiliary electrodes and 0.1 M TBAH electrolyte, was used. The working electrode was cleaned by polishing with 0.3 mm aluminum oxide, followed by sonication, prior to use. In CH_2Cl_2, a Ag/AgI reference electrode (grain of AgI (Fluka)), 0.02 M Bu_4NI (Janssen), and 0.1 M TBAH) was employed. Spectroelectrochemical measurements with the OTTLE cell[6] were performed in CH_2Cl_2 with 0.1 M TBAH by Dr. F. Hartl, University of Amsterdam. Elemental analyses (C, H, S) were carried out on a Carlo Erba NCSO analyzer by the microanalytical department of this university.

[$Me_2Si(\eta^5$-$C_5H_4)_2$]$Fe_2(CO)_4$ (1) can be prepared either photochemically[2] or thermally.[7] Thermal route: A 10.4 g (53.3 mmol) sample of $Fe(CO)_5$ and 5.0 g (26.9 mmol) of $(C_5H_5)_2SiMe_2$ were dissolved in 400 mL of toluene, and the mixture was refluxed for 66 h. The solvent was removed *in vacuo*, and the resulting red oil with red crystalline material was purified by column chromatography (alumina, 5% H_2O; toluene/hexane (1:1)). The first yellow band was discarded. The broad red band was collected, the solvent was evaporated, and the resulting residue was dried *in vacuo* and crystallized from toluene/hexane mixtures. Yield: 5.56 g (50%). IR and ^1H NMR analyses are in accordance with the literature.

[$Me_2Si(\eta^5$-$C_5H_4)_2$]$_2Fe_5S_{12}$ (3) and [$Me_2Si(\eta^5$-$C_5H_4)_2$]$_2Fe_4S_6$ (4). A mixture of 1.60 g of **1** (3.90 mmol) and 1.13 g of S_8 (4.41 mmol) in 400 mL of toluene was refluxed for 69 h. During the reaction, the color changed from dark red to black and a black precipitate was formed. The mixture was filtered, and the residue was extracted with dichloromethane to give product **3** after evaporation of the solvent. The yield after crystallization from dichloromethane/hexane was 0.76 g (0.734 mmol, 47% based on Fe). The filtrate from the reaction mixture was dried *in vacuo*, and the residue was recrystallized from a dichloromethane/hexane mixture to give the black product **4**. The yield after crystallization was 0.73 g (0.926 mmol, 47%). Anal. Calcd (found) for **3**·CH_2Cl_2: C, 26.77 (27.73); H, 2.70 (2.71); S, 34.30 (34.65). Anal. Calcd (found) for **4**: C, 36.56 (36.39); H, 3.58 (3.56); S, 24.40 (25.06). FAB MS for **4**, *m*/*z*: 805 ($[M + OH]^+$, 4%); 788 (M^+, 88%); 756 ($[M - S]^+$, 18%); 724 ([M − 2S], 32%). FD MS for **3**, *m*/*z*: 1035 ($M^+ - 1$).

[$Me_2Si(\eta^5$-$C_5H_4)_2$]$_2Fe_4S_6$(CO) (5). A mixture of 0.95 g of **1** (2.32 mmol) and 0.84 g of S_8 (3.28 mmol) in 400 mL of toluene was cooled to 0 °C and irradiated with a high-pressure mercury lamp for 10 h. The reaction mixture slowly changed color from dark red to black, and an insoluble precipitate formed on the lamp. The mixture was filtered to remove any insoluble material. The filtrate was evaporated to dryness, and the resulting black solid was purified by column chromatography (alumina, 5% H_2O, toluene/hexane (1:1)). The first eluted, dark red, band contained the starting material **1**; then pure toluene was used as eluent and a second, black, band was collected, evaporated to dryness, and recrystallized from CH_2Cl_2/hexane. Yield: 0.4 g (0.5 mmol, 40%). Anal. Calcd (found) for **5**·CH_2Cl_2: C, 34.65 (34.35); H, 3.35 (3.70); S, 21.34 (21.40). FAB MS for **5**, *m*/*z*: 788 ($[M - CO]^+$, 2%); 756 ($[M - S - CO]^+$, 28%); 724 ($[M - 2S - CO]^+$, 19%); 692 ($[M - 3S - CO]^+$, 7%). FD MS for **5**, *m*/*z*: 816 (M^+, 100%); 788 ($[M - CO]^+$, 20%); 756 ($[M - S - CO]^+$, 10%).

[4]PF_6. Method A. A sample of 0.15 g (0.19 mmol) of **4** was dissolved in 30 mL of dichloromethane, and the solution was cooled to 0 °C. Then 0.07 g (0.19 mmol) of [Fc]PF_6 was added, and the reaction mixture was allowed to warm to room temperature, and was stirred for 24 h. Subsequently, 10 mL of hexane was added, and the resulting black precipitate was filtered off, washed with hexane, and dried *in vacuo*. CV showed the product to be pure [**4**]PF_6.

Method B. A sample of 0.05 g (0.063 mmol) of **4** was slurried in acetonitrile, and 0.06 g (0.38 mmol) of NH_4PF_6 was added. This mixture was then exposed to air and was stirred for 24 h, during which the compound slowly dissolved. After addition of 25 mL of dichloromethane, the mixture was filtered to yield a white residue and a black filtrate. The filtrate was evaporated to dryness. The resulting black solid was pure [**4**]PF_6 according to CV.

[3]PF_6 can be prepared in the same way as [**4**]PF_6, but also by controlled-potential bulk electrolysis. In a typical experiment, 38.5 mg of **3** was dissolved in dichloromethane, and the solution was placed in a standard electrolysis unit, with a solution of $Fe(dtc)_3$ in the counter electrode compartment in order to lower the cell potential. The potential of the working electrode was just above the first oxidation potential, and the passed charge was measured until the anodic current was less than 1% of its initial value. The calculated molecular mass of **3** was 1050 ± 50 amu (theoretical value 1036 amu).

[4]$(PF_6)_2$. A sample of 84 mg (0.107 mmol) of **4** was dissolved in 35 mL of dichloromethane, and the solution was cooled to 0 °C. Approximately 30 μL (0.6 mmol) of Br_2 was added with a syringe, and the reaction mixture was stirred for 5 min. A brown precipitate formed, which was filtered off in air, washed with CH_2Cl_2 and heptane, and dried in air. CV in acetonitrile showed it to be a mixture of **[4]**Br_2 and impurities. Yield: 80 mg (80%). The brown powder was dissolved in demineralized water, the mixture was filtered, and the filtrate was added to a saturated KPF_6 solution in water. Within 1 min, a brown precipitate was formed. This was filtered off, washed with water and diethyl ether, and dried in air. Crystallization of crude [**4**]$(PF_6)_2$ from an acetone/diethyl ether mixture in air yielded [**4**]PF_6.

Conversion of 5 to 4. A sample of 56.6 mg (0.0693 mmol) of **5** was dissolved in 50 mL of toluene, and the solution was refluxed for 8 h. The solvent was removed *in vacuo*, and the resulting black solid was crystallized from CH_2Cl_2. After filtration, the mother liquor was evaporated to dryness (fraction 1). The residue was redissolved in a small amount of CH_2Cl_2, and a large amount of hexane was added. The resulting precipitate was filtered off and dried *in vacuo* (fraction 2). Both fractions proved to be pure **4** according to CV and ^1H NMR spectroscopy. The combined yield was quantitative. The conversion of **5** to **4** can be followed by ^1H NMR spectroscopy in a sealed NMR tube at 100 °C.

Attempted Reaction of 4 with PPh_3. A 53.4 mg sample of **4** (0.068 mmol) and 103 mg of PPh_3 (0.39 mmol) were dissolved in 50 mL of toluene. This solution was refluxed for 32 h, after which the solvent was removed *in vacuo*. The only product identified (^1H NMR) was **4**. The reaction was followed with IR spectroscopy. No P═S[8] vibration was observed throughout the experiment.

Structure Determination of 3. Crystals of **3**·CH_2Cl_2 were grown from dichloromethane/hexane mixtures. The black crystals were of poor quality. After thorough inspection, only one crystal was considered to be useful. The crystal (0.12 × 0.26 × 0.24 mm) was mounted in a glass capillary (sealed under N_2 atmosphere) to prevent decomposition and loss of solvent molecules and used to measure a full sphere of reflection data. The unit cell dimensions were determined from the setting angles of 25 reflections in the range $15° < 2\theta < 25°$. Crystal data are given in Table 1.

There was no decomposition during the time of the measurements until, after 10 713 reflections were measured, the crystal cracked and the measurements were stopped. It was, therefore, not possible to further optimize the cell parameters afterward. The Fe and S atoms were found from an automatic Patterson interpretation (PATTY[9]), followed by a phase refinement procedure to expand the fragment (DIRDIF[10]). A Fourier map showed the presence of a dichloromethane molecule. The structure was refined by full-matrix least-squares

(6) Krejcik, M.; Danek, M.; Hartl, F. *J. Electroanal. Chem. Interfacial Electrochem.* **1991**, *317*, 179−187.
(7) Nelson, G. O.; Wright, M. E. *J. Organomet. Chem.* **1982**, *239*, 353−364.
(8) Kimura, T.; Nagata, Y.; Tsurugi, J. *J. Biol. Chem.* **1971**, *246*, 5140−5146.
(9) Admiraal, G.; Behm, H.; Smykalla, C.; Beurskens, P. T. *Z. Kristallogr.* **1992**, *Suppl. 6*, 522.
(10) Beurskens, P. T.; Admiraal, G.; Beurskens, G.; Bosman, W. P.; Garcia-Granda, S.; Gould, R. O.; Smits, J. M. M.; Smykalla, C. *The DIRDIF program system*; Technical Report of the Crystallography Laboratory; University of Nijmegen: Nijmegen, The Netherlands, 1992.
(11) Sheldrick, G. M. *SHELXL-93, Program for the Refinement of Crystal Structures*; University of Göttingen: Göttingen, Germany, 1992.

Table 1. Crystallographic Data for $[Me_2Si(\eta^5\text{-}C_5H_4)_2]_2Fe_5S_{12}\cdot CH_2Cl_2$ (**3**·CH_2Cl_2) and $[Me_2Si(\eta^5\text{-}C_5H_4)_2]_2Fe_4S_6$ (**4**)

	3·CH_2Cl_2	**4**
empirical formula	$C_{25}H_{30}Cl_2Fe_5S_{12}Si_2$	$C_{24}H_{28}Fe_4S_6Si_2$
fw	1121.544	788.40
space group	*C*2/*c* (No. 15)	$P\bar{1}$ (No. 2)
T (K)	293(2)	208(2)
a (Å)	23.480(13)	8.4787(7)
b (Å)	11.192 (4)	12.9648(9)
c (Å)	17.84 (3)	13.4990(9)
α (deg)		79.857(8)
β (deg)	118.58(9)	75.293(8)
γ (deg)		74.041(11)
V (Å^3)	4118(7)	1370.9(2)
Z	4	2
D_{calc} (g/cm^3)	1.809	1.910
radiation	Mo Kα	Mo Kα
μ(Mo Kα) (cm^{-1})	25.173	26.36
no. of reflns collected	10311	5957
R_{merge} (on F_o^2 values)	0.096[a] (0.166)[b]	0.017[a] (0018)[b]
no. of indep reflns	1924[a] (3610)[b]	4407[a] (5957)[b]
R[c]	0.078[a] (0.172)[b]	0.0447[a] (0.0627)[b]
wR_2[d]	0.195[a] (0.374)[b]	0.1230[a] (0.1352)[b]
GOF[e]	1.150[a] (1.604)[b]	1.058[a] (1.058)[b]

[a] $F_o^2 > 2\sigma(F_o^2)$; $F_o > 4\sigma(F_o)$. [b] All data. [c] $R = \sum||F_o| - |F_c||/\sum|F_o|$. [d] $wR_2 = \{\sum[w(F_o^2 - F_c^2)^2]/\sum[w(F_o^2)^2]\}^{1/2}$. [e] GOF $= \{\sum[w(F_o^2 - F_c^2)^2/(n - p)\}^{1/2}$; n = number of reflections and p = total number of parameters.

methods on F^2 values using SHELXL[11] with anisotropic parameters for the non-hydrogen atoms. Hydrogen atoms were included at calculated positions (H in C_5H_4 in riding mode, H in CH_3 as rigid groups). The solvent molecules (CH_2Cl_2) were found at the initial stages of the analysis. Their presence was verified with the "bypass" procedure using the program PLATON.[12] The large anisotropy of the solvent molecules is ascribed to disorder. We were able to split the atomic positions of dichloromethane into the positions for two disordered molecules of idealized geometry. These molecules were refined as rigid groups. The refinement was continued using geometrical restraints for the cyclopentadienyl fragments (maintaining *mm*2 (C_{2v}) symmetry). The refinement converged to an *R* value of 0.078 on *F* values for 1924 observed reflections ($F_o > 4\sigma(F_o)$), with 209 parameters and 31 restraints. The function minimized was $\sum w(F_o^2 - F_c^2)^2$ with $w = 1/[\sigma^2(F_o^2) + (0.089F_o^2)^2]$.

Structure Determination of 4. Suitable crystals of **4** were grown from THF/hexane mixtures at approximately 30 °C. A crystal (0.40 × 0.20 × 0.03 mm) was mounted on a glass fiber, coated with α-cyanoacrylate, and cooled in a stream of N_2. The unit cell dimensions were determined from the setting angles of 25 reflections in the range $15° < 2\theta < 25°$. Crystal data are given in Table 1. A detailed description of the data collection and reduction procedures is given elsewhere.[13] The structure was solved by the program system DIRDIF[10] using the program PATTY[9] to locate the heavy atoms. The hydrogen atoms of the methyl groups were refined as rigid rotors with idealized sp^3 hybridization and a C−H bond length of 0.97 Å to match maximum electron density in a difference Fourier map. All other hydrogen atoms were placed at calculated positions and were subsequently refined as riding on the parent atoms. Calculations with PLATON[12] revealed no higher symmetry and no solvent-accessible areas.

Results and Discussion

Thermal Synthesis of $[Me_2Si(\eta^5\text{-}C_5H_4)_2]_2Fe_5S_{12}$ (3) and $[Me_2Si(\eta^5\text{-}C_5H_4)_2]_2Fe_4S_6$ (4). Compound **1** was synthesized by a modified literature procedure.[7] The thermal reaction of **1** with S_8 (Scheme 1) was followed by means of IR spectroscopy. The CO vibrations of **1** gradually disappeared, and no intermediate carbonyl-containing product could be detected. During the reaction, the color of the reaction mixture slowly changed from dark red to black, and a black precipitate (**3**) was formed. Compound **4** was obtained from the deeply colored filtrate. Compounds **3** and **4** were obtained as pure black crystalline compounds by recrystallization from dichloromethane/hexane.

Scheme 1

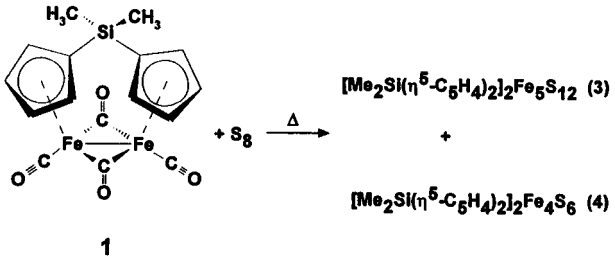

Scheme 2

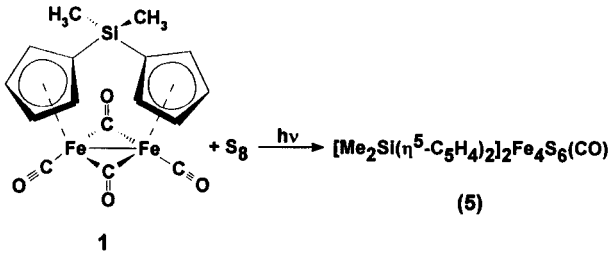

In the FD mass spectrum, a parent ion peak for **3** is found at 1035 amu ($M^+ - 1$). The FAB mass spectrum of **4** revealed the expected value (788 amu) for the parent peak. The isotope distribution around the parent peak and the decomposition pattern point to a product with composition $[Me_2Si(\eta^5\text{-}C_5H_4)_2]_2Fe_4S_6$.

Photochemical Synthesis of $[Me_2Si(\eta^5\text{-}C_5H_4)_2]_2Fe_4S_6(CO)$ (5). A mixture of **1** and an excess of S_8 in toluene was irradiated for 10 h with a high-pressure mercury lamp (Scheme 2). The resulting reaction mixture was filtered and the solvent of the filtrate was removed. After purification of the black residue by column chromatography and subsequent crystallization, the new iron−sulfur cluster compound **5** was obtained.

The infrared spectrum shows an absorption band at 1923 cm^{-1}, and the ^{13}C NMR spectrum contains a resonance signal at $\delta = 220.7$ ppm. These spectroscopic data strongly point to the presence of a terminal CO ligand in the cluster compound. The FD mass spectrum of **5** shows the expected parent ion peak M^+ at 816 amu, although its intensity is only about 20% of the $[M - CO]^+$ peak at 788 amu. Unfortunately, attempts to obtain suitable crystals for X-ray structure analysis have failed thus far. The composition of **5** was however confirmed by thermoanalysis. After heating of **5** in toluene, the *only* product identified was **4,** in virtually 100% yield. This confirms that **5** is an Fe_4S_6 cluster with an additional CO ligand. Further evidence for the presence of a terminal carbonyl ligand was obtained from IR spectroelectrochemical measurements (*vide infra*). The photochemical reaction of $(\eta^5\text{-}C_5H_4R)Fe_2(CO)_4$ with S_8 in methanol has been reported to give $(\eta^5\text{-}C_5H_4R)_2Fe_2S_5(CO)_4$, $(\eta^5\text{-}C_5H_4R)_2Fe_2S_4(CO)$, and $(\eta^5\text{-}C_5H_4R)_2Fe_2S_4$ as consecutive products.[14]

Molecular Structures. a. $[Me_2Si(\eta^5\text{-}C_5H_4)_2]_2Fe_5S_{12}$ (3). Crystals of **3**·CH_2Cl_2 suitable for X-ray structure analysis were obtained by slow diffusion of hexane into a dichloromethane solution during a short period (1 week at room temperature). Earlier attempts to crystallize **3** from CH_2Cl_2/hexane mixtures

(12) Spek, A. L. *Acta Crystallogr.* **1990**, *A46*, C34.
(13) Smits, J. M. M.; Behm, H.; Bosman, W. P.; Beurskens, P. T. *J. Crystallogr. Spectrosc. Res.* **1988**, *18*, 447−450.
(14) Chanaud, H.; Ducourant, A. M.; Giannotti, C. *J. Organomet. Chem.* **1980**, *190*, 201−216.

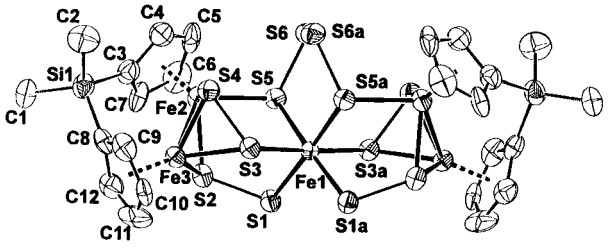

Figure 1. X-ray structure of $[Me_2Si(\eta^5\text{-}C_5H_4)_2]_2Fe_5S_{12}$ (**3**). Hydrogen atoms are omitted for clarity, and thermal ellipsoids are at 50% probability.

Table 2. Interatomic Distances (Å) for Compound **3**

Fe(1)−S(1)	2.226(5)	Fe(2)−Fe(3)	2.550(3)
Fe(1)−S(3)	2.275(5)	S(1)−S(2)	2.067(7)
Fe(1)−S(5)	2.278(5)	S(3)−S(4)	2.065(6)
Fe(2)−S(4)	2.193(5)	S(5)−S(6)	2.100(6)
Fe(2)−S(5)	2.243(6)	S(6)−S(6a)	2.019(9)
Fe(2)−S(2)	2.245(5)	Fe(2)−Cp(2)[a]	1.723(9)
Fe(3)−S(4)	2.170(5)	Fe(3)−Cp(3)[a]	1.711(7)
Fe(3)−S(2)	2.175(5)	Si(1)−Cp(2)[a]	0.109(29)
Fe(3)−S(3)	2.291(6)	Si(1)−Cp(3)[a]	0.311(25)

[a] Distance to least-squares plane through carbons of Cp(*n*). Cp(*n*) = η^5-C_5H_4 attached to Fe(*n*).

Table 3. Angles (deg) for Compound **3**

S(1a)−Fe(1)−S(1)	98.7(3)	S(5)−Fe(2)−S(2)	85.4(2)
S(1a)−Fe(1)−S(3)	90.3(2)	S(2)−Fe(2)−Fe(3)	53.49(12)
S(1)−Fe(1)−S(3)	91.3(2)	S(4)−Fe(3)-S(2)	102.4(2)
S(3a)−Fe(1)−S(3)	177.6(3)	S(4)−Fe(3)−Fe(2)	54.66(13)
S(1)−Fe(1)−S(5a)	175.33(13)	S(3)−Fe(3)−Fe(2)	86.46(14)
S(3)−Fe(1)−S(5a)	84.1(2)	S(2)−Fe(3)−S(3)	91.2(2)
S(1a)−Fe(1)−S(5)	175.32(13)	C(8)−Si(1)−C(1)	111.3(8)
S(1)−Fe(1)−S(5)	81.4(2)	C(8)−Si(1)−C(3)	105.1(7)
S(3a)−Fe(1)−S(5)	84.1(2)	C(1)−Si(1)−C(3)	109.9(8)
S(3)−Fe(1)−S(5)	94.4(2)	C(8)−Si(1)−C(2)	107.5(8)
S(5a)−Fe(1)−S(5)	98.8(2)	C(1)−Si(1)−C(2)	113.4(10)
S(4)−Fe(2)−S(5)	90.3(2)	C(3)−Si(1)−C(2)	109.3(8)
S(4)−Fe(2)−S(2)	99.4(2)	Cp(2)−Cp(3)[a]	99.4(7)

[a] Angle between least-squares planes through carbons of Cp(*n*). Cp(*n*) = η^5-C_5H_4 attached to Fe(*n*).

at elevated temperatures over a longer period (8 weeks) had resulted in oxidative decomposition of **3**, yielding $\mathbf{3}^+[FeCl_4]^-$.[2]

The geometry of **3** (Figure 1, Tables 2 and 3) differs only slighly from the geometry of $\mathbf{3}^+$.[2]

The unit cell of $\mathbf{3}\cdot CH_2Cl_2$ contains both enantiomers of the chiral molecule, each situated around a crystallographic 2-fold axis through the central iron atom.

The Fe_5S_{12} cores of **3** and $\mathbf{3}^+$ have a bowtie shape.[15−19] For iron−sulfur clusters only a few examples of such a shape have been reported to date.[20−22] Compound **3** consists of a central Fe atom linked via one tetrasulfido and four disulfido fragments to two $Me_2Si(\eta^5\text{-}C_5H_4)_2Fe_2$ moieties (Figure 1). The tetrasulfido ligand bridges the central iron atom and the $Me_2Si(\eta^5\text{-}C_5H_4)_2Fe_2$ moieties in a μ_2:μ_2-bonding mode.

The central iron atom is almost ideally octahedrally coordinated by six sulfur atoms. The Fe−S bond lengths of the central iron atom range from 2.23 to 2.28 Å and are well within the range observed for other Fe−S distances in octahedral complexes in which Fe has a formal oxidation state of II.[23−25] Although small, the structural deviations on going from **3** to $\mathbf{3}^+$ are the largest for the FeS_6 cores, thus indicating Fe(1) as the formal Fe(III) center in $\mathbf{3}^+$.

The S−S distances in the tetrasulfido group are in the range 2.02−2.10 Å. This dispersion has been found for other tetrasulfido ligands.[26]

The occurrence of the tetrasulfido group is unprecedented for iron−sulfur clusters. Sulfur is known to form catenanes, including the S_4^{2-} anion, in a large number of compounds.[27−32] Thus far, no η^5-Cp iron−sulfur clusters with S_x groups, $x > 2$, have been reported.

In the $Me_2Si(\eta^5\text{-}C_5H_4)_2Fe_2$ units, each iron is coordinated by three sulfur atoms and one C_5H_4 ring. The angle between the least-squares planes of the C_5H_4 rings is 99°. This is almost identical to the value in the starting material **1** (97°), which suggests that the strain in the bridging $Me_2Si(\eta^5\text{-}C_5H_4)$ ligand does not increase on going from **1** to **3**. The Fe(2)−Fe(3) distance (2.55 Å) is short compared to the distances in known cyclopentadienyl iron−sulfur cluster compounds without a Cp−Cp linkage[33] (average 2.65 Å) and is close to the value in the starting material **1** (2.51 Å). The coordination geometry around the Si atom is that of a slightly distorted tetrahedron. The Fe−S distances to the $[Me_2Si(\eta^5\text{-}C_5H_4)_2]Fe_2$ units range from 2.17 to 2.29 Å and are normal values for Fe−S distances in iron−sulfur cluster compounds.[34−36]

b. $[Me_2Si(\eta^5\text{-}C_5H_4)_2]_2Fe_4S_6$ (4). Crystals of **4** suitable for X-ray diffraction were grown from THF/hexane. The molecular structure of this cluster is shown in Figure 2. The molecule exhibits almost perfect C_2 symmetry in the solid state (see Tables 4 and 5).

The structure of **4** is very similar to that of $Cp_4Fe_4S_6$.[33,37] The Fe(1)−Fe(2) and Fe(3)−Fe(4) distances are 2.62 and 2.63

(15) Eremenko, I. L.; Pasynskii, A. A.; Gasanov, G. S.; Orazsakhatov, B.; Struchkov, Y. T.; Shklover, V. E. *J. Organomet. Chem.* **1984**, *275*, 183−189.
(16) Vahrenkamp, H.; Dahl, L. F. *Angew. Chem.* **1969**, *81*, 152−153.
(17) Pasynskii, A. A.; Eremenko, I. L.; Orazsakhatov, B.; Gasanov, G. S.; Shklover, V. E.; Struchkov, Y. T. *J. Organomet. Chem.* **1984**, *269*, 147−153.
(18) Eremenko, I. L.; Pasynskii, A. A.; Gasanov, G. S.; Orazsakhatov, B.; Struchkov, Y. T.; Shklover, V. E. *J. Organomet. Chem.* **1984**, *275*, 71−81.
(19) Pasynskii, A. A.; Eremenko, I. L.; Gasanov, G. S.; Struchkov, Y. T.; Shklover, V. E. *J. Organomet. Chem.* **1984**, *276*, 349−362.
(20) Barber, D. E.; Sabat, M.; Sinn, E.; Averill, B. A. *Organometallics* **1995**, *14*, 3229−3237.
(21) Holliday, R. L.; Roof, L. C.; Hargus, B.; Smith, D. M.; Wood, P. T.; Pennington, W. T.; Kolis, J. W. *Inorg. Chem.* **1995**, *34*, 4392−4401.
(22) Calderoni, F.; Demartin, F.; Iapalucci, M. C.; Laschi, F.; Longoni, G.; Zanello, P. *Inorg. Chem.* **1996**, *35*, 898−905.
(23) Sellmann, D.; Mahr, G.; Knoch, F. *Angew. Chem.* **1991**, *103*, 1493−1495.
(24) Sellmann, D.; Geck, M.; Knoch, F.; Ritter, G.; Dengler, J. *J. Am. Chem. Soc.* **1991**, *113*, 3819−3828.
(25) Sellmann, D.; Mahr, G.; Knoch, F. *Inorg. Chim. Acta* **1994**, *224*, 35−43.
(26) Fedin, V. P.; Sokolov, M. N.; Geras'ko, O. A.; Sheer, M.; Fedorov, V. Y.; Mironov, A. V.; Slovokhotov, Y. L.; Struchkov, Y. T. *Inorg. Chim. Acta* **1989**, *165*, 25−26.
(27) Müller, A.; Diemann, E. *Adv. Inorg. Chem.* **1987**, *31*, 89−122.
(28) Müller, A.; Schimanski, J.; Römer, M.; Bögge, H.; Baumann, F.-W.; Eltzner, W.; Krickemeyer, E.; Billerbeck, U. *Chimia* **1985**, *39*, 25−27.
(29) Müller, A.; Krickemeyer, E.; Bögge, H.; Penk, M.; Rehder, D. *Chimia* **1986**, *40*, 50−52.
(30) Müller, A.; Baumann, F.-W.; Bögge, H.; Römer, M.; Krickemeyer, E.; Schmitz, K. *Angew. Chem.* **1984**, *96*, 607−608.
(31) Isobe, K.; Ozawa, Y.; Demiguel, A. V.; Zhu, T. W.; Zhao, K. M.; Nishioka, T.; Ogura, T.; Kitagawa, T. *Angew. Chem., Int. Ed. Engl.* **1994**, *33*, 1882−1883.
(32) Tokitoh, N.; Kano, N.; Shibata, K.; Okazaki, R. *Organometallics* **1995**, *14*, 3121−3123.
(33) Vergamini, P. J.; Kubas, G. J. *Prog. Inorg. Chem.* **1976**, *21*, 261−282.
(34) Wei, C. H.; Wilkes, G. R.; Treichel, P. M.; Dahl, L. F. *Inorg. Chem.* **1966**, *5*, 900−905.
(35) Schunn, R. A.; Fritchie, C. J. J.; Prewitt, C. T. *Inorg. Chem.* **1966**, *5*, 892−899.
(36) Kubas, G. J.; Vergamini, P. J. *Inorg. Chem.* **1981**, *20*, 2667−2676.
(37) Behm, H.; Jordanov, J.; Moers, F. G.; Beurskens, P. T. *J. Crystallogr. Spectrosc. Res.* **1991**, *21*, 741−743.

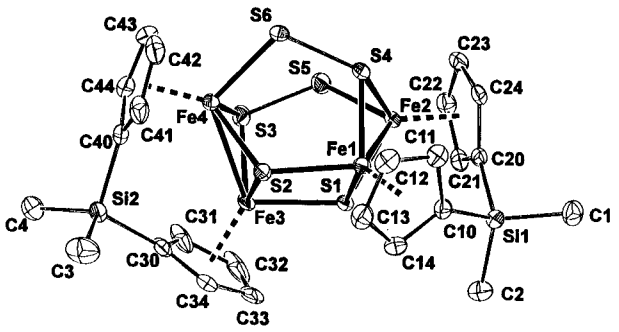

Figure 2. X-ray structure of $[Me_2Si(\eta^5\text{-}C_5H_4)_2]_2Fe_4S_6$ (**4**). Hydrogen atoms are omitted for clarity, and thermal ellipsoids are at 50% probability.

Table 4. Interatomic Distances (Å) for Compound **4**

Fe(1)−Fe(2)	2.6210(9)	Fe(1)−Cp(1)[a]	1.760(4)
Fe(3)−Fe(4)	2.6251(9)	Fe(3)−Cp(1)[a]	1.757(4)
Fe(1)−Fe(3)	3.431 (1)	Fe(2)−Cp(1)[a]	1.755(3)
Fe(2)−Fe(4)	4.368 (1)	Fe(4)−Cp(1)[a]	1.755(3)
Fe(1)−S(1)	2.2167(13)	Fe(1)−C(av)[b]	2.125(5)
Fe(3)−S(2)	2.2158(14)	Fe(3)−C(av)[b]	2.129(6)
Fe(1)−S(2)	2.2658(13)	Fe(2)−C(av)[b]	2.122(5)
Fe(3)−S(1)	2.2409(13)	Fe(4)−C(av)[b]	2.128(5)
Fe(1)−S(4)	2.1816(13)	Si(1)−C(1)	1.858(5)
Fe(3)−S(3)	2.186(2)	Si(2)−C(3)	1.849(6)
Fe(2)−S(1)	2.2021(13)	Si(1)−C(2)	1.864(5)
Fe(4)−S(2)	2.2009(14)	Si(2)−C(4)	1.844(6)
Fe(2)−S(4)	2.2194(13)	Si(1)−C(10)	1.873(5)
Fe(4)−S(3)	2.2132(14)	Si(2)−C(30)	1.859(5)
Fe(2)−S(5)	2.2393(14)	Si(1)−C(20)	1.858(5)
Fe(4)−S(6)	2.2389(13)	Si(2)−C(40)	1.858(5)
S(3)−S(5)	2.034(2)	S(5)−S(6)	3.401 (2)
S(4)−S(6)	2.035(2)		

[a] Distance to least-squares plane through carbons of Cp(*n*). Cp(*n*) = η^5-C_5H_4 attached to Fe(*n*). [b] C of η^5-C_5H_4 fragment.

Table 5. Angles (deg) for Compound **4**

Fe(2)−Fe(1)−S(1)	53.36(4)	Cp(1)−Cp(2)[a]	105.26(20)
Fe(4)−Fe(3)−S(2)	53.27(4)	Cp(3)−Cp(4)[a]	99.29(19)
Fe(2)−Fe(1)−S(2)	108.08(4)	C(1)−Si(1)−C(2)	112.8(3)
Fe(4)−Fe(3)−S(1)	107.78(4)	C(3)−Si(2)−C(4)	112.9(3)
Fe(2)−Fe(1)−S(4)	54.12(4)	C(1)−Si(1)−C(10)	110.9(2)
Fe(4)−Fe(3)−S(3)	53.84(4)	C(3)−Si(2)−C(30)	109.4(3)
Fe(1)−Fe(2)−S(1)	53.88(4)	C(1)−Si(1)−C(20)	108.4(2)
Fe(3)−Fe(4)−S(2)	53.79(4)	C(3)−Si(2)−C(40)	109.5(3)
Fe(1)−Fe(2)−S(4)	52.79(4)	C(2)−Si(1)−C(10)	109.7(2)
Fe(3)−Fe(4)−S(3)	52.88(4)	C(4)−Si(2)−C(30)	111.5(3)
Fe(1)−Fe(2)−S(5)	117.10(4)	C(2)−Si(1)−C(20)	109.7(2)
Fe(3)−Fe(4)−S(6)	117.10(4)	C(4)−Si(1)−C(40)	107.1(3)
Fe(2)−S(5)−S(3)	111.06(7)	C(10)−Si(2)−C(20)	105.1(2)
Fe(4)−S(6)−S(4)	110.98(6)	C(30)−Si(2)−C(40)	106.2(2)

[a] Angle between least-squares planes through carbons of Cp(*n*). Cp(*n*) = η^5-C_5H_4 attached to Fe(*n*).

Å, respectively, close to those in $Cp_4Fe_4S_6$ (2.64 Å). The coordination of the bridging silicon atoms is close to tetrahedral, with the C(10)−Si(1)−C(20) and C(30)−Si(2)−C(40) angles being 6° smaller than the C(1)−Si(1)−C(2) and C(3)−Si(2)−C(4) angles. The angles between the least-square planes of C_5H_4(1) and C_5H_4(2) and between the least-squares planes of C_5H_4(3) and C_5H_4(4) are 105 and 99°, respectively, which are close to the corresponding angle in $Cp_4Fe_4S_6$ (100°). Thus the insertion of a silicon atom between two C_5H_4 rings does not appear to impose much strain on the Fe_4S_6 core. However, it has a drastic influence on the stability of **4** (*vide infra*).

^{1}H NMR and ^{13}C NMR Spectroscopy. In the ^{1}H NMR spectra of **3**−**5**, the resonance signals are found in the expected ranges: the C_5H_4 protons at 3.5−8.0 ppm and the Me_2Si protons from 0.0 to 0.5 ppm (see Table 6).

For **3**, the sixteen C_5H_4 protons provide eight signals with equal intensities and the six protons of the Me_2Si groups give rise to two signals with triple intensities. The number of C_5H_4 resonances reflects the C_2 symmetry of the molecule, in agreement with the X-ray structure analysis.

In accordance with the pseudo-C_2 symmetry of the crystal structure, **4** has six resonance signals with equal intensities and one signal with double intensity for the sixteen C_5H_4 protons. 2D COSY ^{1}H NMR analysis of **4** shows a clear correlation within two sets of C_5H_4 proton signals, ascribed to the two sets of two equivalent C_5H_4 moieties. Upon brief contact of a $CDCl_3$ solution of **4** with air, three of the C_5H_4 proton signals (one having double intensity) in the ^{1}H NMR spectrum broaden (see Figure 3a). When a sample of **4** in $CDCl_3$ is exposed to air for days or when a mixture of **4** and **4**(PF_6) is dissolved in $CDCl_3$ (Figure 3b), the initially broadened C_5H_4 signals in the ^{1}H NMR spectrum broaden further and shift.

Comparison with the 2D COSY ^{1}H NMR of **4** reveals that the sharp signals belong to one C_5H_4 ring and the broadened signals to the other C_5H_4 ring of the $Me_2Si(\eta^5\text{-}C_5H_4)_2$ unit. The broadening can be explained by a weak paramagnetism, due to a small amount of oxidized species, which allows rapid electron exchange with the neutral complex. The preferential broadening of one set of signals indicates that the unpaired electron in $\mathbf{4}^+$ is predominantly localized in the Fe(1)−Fe(3) or the Fe(2)−Fe(4) pair of the Fe_4S_6 cluster. This conclusion is in accordance with Kubas' result, which showed that, upon oxidation of $Cp_4Fe_4S_6$, the electron is taken from an antibonding orbital localized at the iron atoms Fe(1) and Fe(3).[33]

In the ^{1}H NMR spectrum of **5**, thirteen signals with equal intensities and one signal with triple intensity are observed for the C_5H_4 protons and four signals with triple intensities are observed for the methyl protons. In the 2D COSY ^{1}H NMR spectrum, a correlation was found between four sets of ^{1}H resonances. Thus four different C_5H_4 moieties are present in this molecule, in accordance with its lack of symmetry. This lack of symmetry is also confirmed by the ^{13}C NMR spectrum of **5** (Table 6). Fourteen signals between 70 and 105 ppm are observed, one of which has a double intensity. One more resonance is believed to be hidden under the intense signal of $CDCl_3$ (77 ppm). As expected, the resonances of the ipso carbons were not observed. The four methyl signals of the two dimethylsilyl groups are found around 0 ppm. A weak signal at 221 ppm is assigned to the carbonyl group.[38]

Mössbauer Spectroscopy. The data for $\mathbf{3}^z$ and $\mathbf{4}^z$, $z = 0$, $+1$, are assembled in Table 7. The Mössbauer spectrum of **3** reveals a superposition of different iron sites (Figure 4a).

The best fit for **3** is obtained using a 2:2:1 iron site model according to the X-ray structure analysis (Figure 1) and to NMR spectroscopic data. The unique iron atom has an isomer shift of 0.25 mm s^{-1} and a quadrupole splitting of 0.43 mm s^{-1}. The two pairs of iron atoms have very similar quadrupole splittings (1.10 and 1.11 mm s^{-1}) and slightly different isomer shifts (0.25 and 0.35 mm s^{-1}). Upon oxidation of **3** to $\mathbf{3}^+$, the same 2:2:1 Fe site ratio is observed (Figure 4b) but all the signals have shifted. The doublet of the central iron site has shifted to a lower value, consistent with a higher relative s-electron density at the central Fe nucleus caused by the loss of one d electron.[39]

(38) Elschenbroich, C.; Salzer, A. *Organometallics. A concise introduction*; VCH Verlagsgesellschaft mbH: Weinheim, Germany, 1989.

(39) A change in the isomer shift from a high to a low value on going from low-spin Fe(II) to low-spin Fe(III) is generally found in octahedrally coordinated FeS_6 species, although the regions of IS(Fe(III)) and IS(Fe(II)) differ distinctly: Gütlich, P.; Link, R.; Trautwein, A. X. *Mossbauer Spectroscopy and Transition Metal Chemistry*; Springer-Verlag: Berlin, 1978.

Table 6. ^{1}H NMR Data[a] for Compounds **3**, **4**, **5**, and **4**$(PF_6)_2$[b] and ^{13}C NMR Data[c] for Compound **5**

compd		Cp	Si−CH_3	CO
3	^{1}H NMR	5.90 (2); 5.64 (2); 5.36 (2); 5.31 (2); 5.24 (2); 5.05 (2); 4.77 (2); 4.05 (2)	0.32 (6); 0.25 (6)	
4	^{1}H NMR	6.90 (2); 6.11 (2); 5.98 (2); 5.05 (2); 4.59 (2); 4.41 (4); 3.71 (2)	−0.01 (6); 0.10 (6)	
4$(PF_6)_2$	^{1}H NMR	7.96 (2); 6.72 (2); 6.58 (2); 6.19 (2); 5.68 (2); 5.08 (2); 4.97 (2); 4.62 (2)	0.29 (6); 0.15 (6)	
5	^{1}H NMR	5.57 (1); 5.45 (1); 5.23 (1); 5.18 (1); 5.11 (1); 5.05 (1); 4.98 (1); 4.88 (1); 4.73 (1); 4.69 (1); 4.66 (1); 4.54 (1); 4.36 (3); 3.90 (1)	0.51 (3); 0.46 (3); 0.32 (3); 0.15 (3)	
5	^{13}C NMR[d]	102.2; 99.6; 97.1; 93.2; 92.3; 91.0; 90.3; 89.8; 88.0; 84.1; 83.9; 83.6; 75.1; 74.0	−1.4; −1.7; −2.2; −2.9	220.7

[a] $CDCl_3$ (7.29 ppm) solutions at 298 K. Integrations are given in parentheses. No clear couplings could be observed. [b] CD_3CN (2.01 ppm) solution at 298 K. [c] $CDCl_3$ (77.0 ppm) solution at 298 K. [d] Quarternary carbons are not observed.

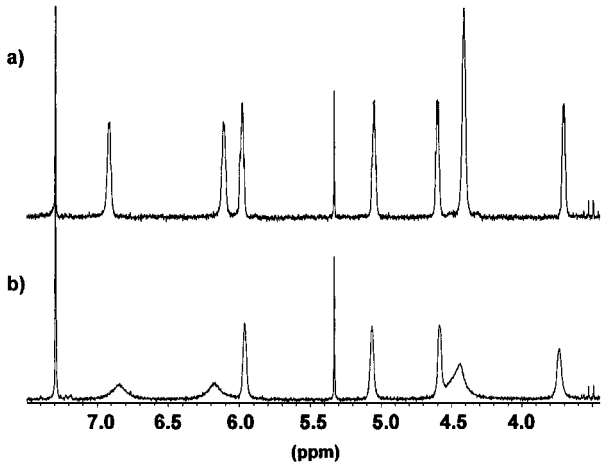

Figure 3. ^{1}H NMR spectra in $CDCl_3$ at 200 MHz: (a) **4** after brief contact with air; (b) a mixture of **4** and **4**(PF_6).

Table 7. Mössbauer Data for Iron−Sulfur Cluster Compounds

compd	fraction (%)	IS ($mm\cdot s^{-1}$)[a]	QS ($mm\cdot s^{-1}$)	Γ ($mm\cdot s^{-1}$)
3	40	0.25	1.10	0.34
	40	0.35	1.11	0.34
	20	0.25	0.43	0.34
3$^+$	40	0.22	1.07	0.29
	40	0.42	1.09	0.29
	20	0.16	1.53	0.29
4		0.34	1.02	0.27
4$^+$		0.31	0.96	0.25

[a] Vs α-Fe at room temperature.

The doublet of one of the two two-iron sites also shifts to lower values, albeit to a lesser extent, whereas the doublet of the other two-iron site shifts to higher values. The most remarkable result of the Mössbauer studies is the minor change of the quadrupole splitting of the two two-iron sites upon oxidation, whereas the QS of the central iron atom changes substantially, in accordance with the change from low-spin Fe(II) to low-spin Fe(III) in octahedral coordination.[40,41]

The Mössbauer spectra for **4** and [**4**]PF_6 are almost identical and consist of one doublet, implying that the Fe sites are identical. This is obviously not true from a structural point of view, but Mössbauer spectroscopy appears to be unable to distinguish between the various Fe sites. The spectra reported for $Cp_4Fe_4S_6^{0/+}$ (recorded at 4 K) also show one doublet, but the data were fitted in accordance with a two-site model.[42] The value for the IS of **4** is lower than that found for $Cp_4Fe_4S_6$.

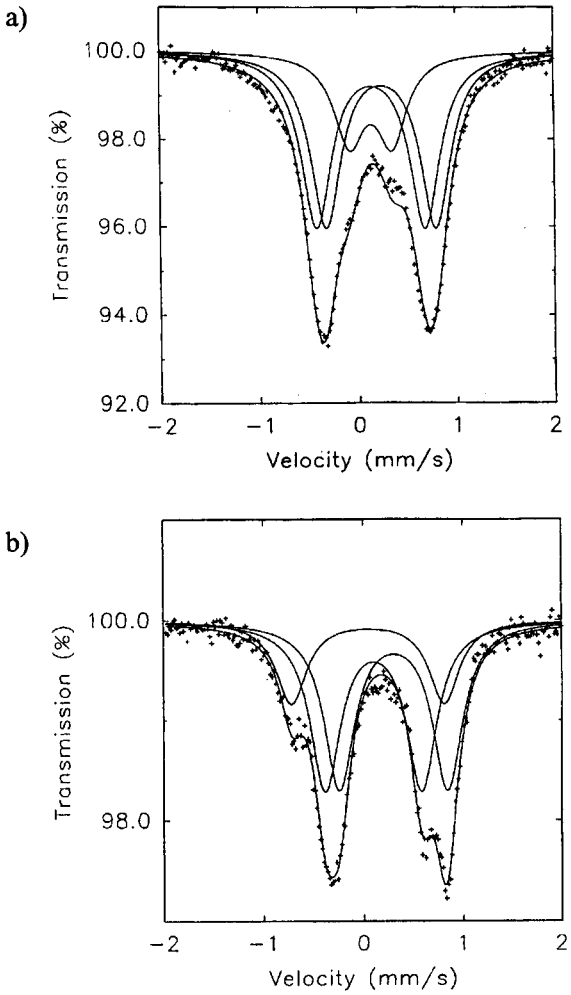

Figure 4. Mössbauer spectra of (a) **3** and (b) **3**(PF_6), recorded at 77 K.

This could be due to the different temperatures at which **4** (298 K) and $Cp_4Fe_4S_6$ (4 K) have been measured.[25] The almost negligible changes in the spectra upon going from **4** to **4**$^+$ seem to indicate that changes in electron density upon oxidation are counteracted by structural changes, as has been postulated for the $Cp_4Fe_4S_4^{+/2+}$ series,[43] or that the oxidation step is cyclopentadienyl ligand based.[43,44] In η^5-Cp iron−sulfur clusters, a change of oxidation state is often accompanied by a very small change in isomer shift.[43]

Redox Behavior and Spectroelectrochemical Measurements. Redox potentials of **3**−**5** are listed in Table 8, together with those of some other iron−sulfur clusters. All potentials are quoted *vs* the potential of the Fc/Fc^+ redox couple.

(40) An increase in the QS on going from low-spin Fe(II) to low-spin Fe(III) in an octahedral coordination is found for $M_x[Fe(CN)_6]$ (M = Na, K; x = 4, 3), although to a lesser extent: Drago, R. S. *Physical Methods in Chemistry*; W. B. Saunders Co.: Philadelphia, PA, 1977; p 541.

(41) Kuppers, H.-J.; Wieghardt, K.; Nuber, B.; Weiss, J.; Bill, E.; Trautwein, A. X. *Inorg. Chem.* **1987**, *26*, 3762−3769.

(42) Dupré, N. Thesis, University of Grenoble, Grenoble, France, 1986.

(43) Wong, H.; Sedney, D.; Reiff, W. M.; Frankel, R. B.; Meyer, T. J.; Salmon, D. *Inorg. Chem.* **1978**, *17*, 194−197.

(44) Bernal, I.; Davis, B. R.; Good, M. L.; Chandra, S. *J. Coord. Chem.* **1972**, *2*, 61−65.

Table 8. Redox Potentials for Complexes **3**, **4**, **5**, and Related Compounds[a]

	$E_{1/2}$ (V) (ΔE_p (mV))				
complex	−1/0	0/+1	+1/+2	+2/+3	+3/+4
3	−1.53 (60)	−0.41 (56)	0.49[b]		
4	−1.75 (60)	−0.45 (57)	0.14 (57)	0.80[b]	1.02[b]
5	−1.62 (58)	−0.38 (57)	−0.01 (58)	0.80 (38)[f]	
$Cp_4Fe_4S_4$[c]		−0.73	−0.04		
$Cp_4Fe_4S_5$[d]	−1.76	−0.62	−0.30	0.73	
$Cp_4Fe_4S_6$[d]	−1.72	−0.45	−0.14	0.85[b]	
$[Me(\eta^5\text{-}C_5H_4)]_4Fe_4S_4$[e]		−0.83	−0.10		
$[Me(\eta^5\text{-}C_5H_4)]_4Fe_4S_6$[e]	−1.89	−0.57	−0.24	0.86[b]	

[a] CH_2Cl_2 solutions with 0.1 M TBAH as supporting electrolyte. Potentials versus Fc/Fc^+. Peak separations are given in parentheses. [b] Peak potential. [c] From literature.[62,63] [d] From literature.[36,62] [e] From literature.[51] [f] Adsorption phenomenon.

The Fe_5S_{12} cluster compound **3** exhibits a reversible reduction (0/−1) and oxidation (0/+1) and an irreversible +1/+2 oxidation. The second oxidation occurs at approximately 900 mV higher potential than the first. This redox behavior differs somewhat from that of the Fe_4S_6 cubane-type clusters **4** and **5**. The redox behavior of **4** and **5** is characteristic of cyclopentadienyl iron−sulfur cubane-type cluster compounds and resembles strongly that of analogous clusters with nonbridged cyclopentadienyl groups, $Cp_4Fe_4S_6$ and $Cp_4Fe_4S_5$. In CH_2Cl_2, **4** undergoes two reversible oxidations, separated by 600 mV, two irreversible oxidations, and one reversible reduction. Compound **5** shows three reversible oxidations and one reversible reduction. There is a striking similarity between the redox potentials of compound **4** and its nonbridged analog, $Cp_4Fe_4S_6$. Except for the second oxidation, all redox potentials of **4** are within 50 mV of those for $Cp_4Fe_4S_6$. Apparently, the bridging $SiMe_2$ group has little influence on the electronic properties of this cluster in the oxidation states −1, 0, and +1. This parallels the electronic influence of the $SiMe_3$ group in sandwich complexes.[45] In the Fe_4S_6 compound $[(\eta^5\text{-}C_5H_4)SiMe_3]_4Fe_4S_6$, however, the $SiMe_3$ group is believed to be electron-donating, causing a negative shift in redox potentials.[46] In compound **4**, the ligand seems to be responsible for the shift of the +1/+2 transition: steric constraints within the bridging dicyclopentadienyl ligand might hamper the oxidation step +1/+2.

The redox potentials of the cluster compounds depend on the solvent used. For example, on going from CH_2Cl_2 to DMF, the +1/+2 transition of **4** shifts 100 mV in the negative direction, indicating an increasing cluster ion−solvent interaction.

The redox behavior of **5** differs from that of **4** despite the fact that both compounds contain an Fe_4S_6 core. The redox potentials of the −1/0 and 0/+1 transitions are shifted to slightly more positive values with respect to the corresponding redox processes of **4**, perhaps due to the electron-withdrawing nature of bonded CO. In contrast, the redox pair +1/+2 is shifted about 150 mV in the negative direction with respect to **4**. The redox wave +2/+3 shows a characteristic feature indicating adsorption phenomena of the oxidized compound on the surface of the electrode.

In infrared spectroelectrochemical measurements, the energy of the CO stretching vibration of **5** in CH_2Cl_2 was found to increase in steps of 22, 32, and 34 cm^{-1}, respectively, on passing through the cluster oxidation states −1 (1901 cm^{-1}), 0 (1923 cm^{-1}), +1 (1955 cm^{-1}), and +2 (1989 cm^{-1}). For the trication, no ν_{CO} was observed, probably because CO dissociates at this oxidation state, although the 2+/3+ redox transition was found to be reversible (*vide supra*). The shifts in ν_{CO} are in agreement with a strengthening of the C−O bond upon decrease of electron density available for π back-donation. The sensitivity of carbonyl ligands to (partial) electron transfer has been well documented.[47−49]

Table 9. EPR Data for $\mathbf{3}^+$, $\mathbf{4}^+$, and $\mathbf{5}^+$

	g_1[c]	g_2[c]	g_3[c]	$\langle g \rangle$
$\mathbf{3}^+$ [a]	2.418	2.123	1.980	2.193
$\mathbf{4}^+$ [a]	2.094	2.003	1.982	2.026
$\mathbf{5}^+$ [b]	2.061	2.037	1.997	2.032

[a] Obtained from $CHCl_3$/DMF (1/1) solutions of the PF_6 salts at T = 110K. [b] Obtained *in situ* by means of controlled-potential electrolysis in DMF, measured at 8 K. [c] $g_i \pm 0.001$.

EPR Spectroscopy. Frozen-solution EPR spectra of $\mathbf{3}^+$ and $\mathbf{4}^+$ were obtained from DMF/$CHCl_3$ solutions of the PF_6 salts. The frozen-solution spectrum of $\mathbf{5}^+$ was recorded after generation in situ by controlled-potential electrolysis in an EPR tube.[50] All three spectra reveal three different g values (Table 9), consistent with a rhombic **g** tensor of a low-spin $S = {}^1/_2$ system.

For $\mathbf{4}^+$ and $\mathbf{5}^+$, a small g anisotropy is found, in agreement with observations for other cubane-type $[Cp_4Fe_4S_x]$ radical complexes.[42,51−54] The g anisotropy of $\mathbf{3}^+$ is considerably more pronounced. This is in accordance with the virtually octahedrally coordinated central iron atom being the paramagnetic center.[55,56]

Reactivity. As mentioned above, **3** appeared to be reactive toward freshly distilled dichloromethane, as is well established for other sulfido group containing complexes.[57,58] The dichloromethane used was freed from radical inhibitor; therefore, chlorine radicals are held responsible for the oxidation of part of **3** to $\mathbf{3}^+$ and the decomposition of another part to yield the $FeCl_4^-$ anion. The resulting salt [**3**]$FeCl_4$ precipitated.[2]

Surprisingly, **4** is thermally very stable and is recovered unchanged after refluxing in toluene for 32 h, even in the presence of an excess of triphenylphosphine. In marked contrast to **4**, $Cp_4Fe_4S_6$ loses elemental sulfur upon heating, ultimately yielding $Cp_4Fe_4S_4$.[33]

As can be deduced from their cyclic voltammograms, compounds **3** and **4** can be oxidized to their monocations at mild potentials. [**3**]PF_6 and [**4**]PF_6 were obtained by use of air or [Fc]PF_6 as oxidants. The redox behavior of **4** indicates that **4** can be oxidized to the dication by a powerful oxidant. Indeed,

(45) Lu, S. X.; Strelets, V. V.; Ryan, M. F.; Pietro, W. J.; Lever, A. B. P. *Inorg. Chem.* **1996**, *35*, 1013−1023.
(46) Yamada, M.; Tobita, H.; Inomata, S.; Ogino, H. *Bull. Chem. Soc. Jpn.* **1996**, *69*, 861−867.
(47) Anson, C. E.; Creaser, C. S.; Stephenson, G. R. *J. Chem. Soc., Chem. Commun.* **1994**, 2175−2176.
(48) Lorkovic, I. M.; Wrighton, M. S.; Davis, W. M. *J. Am. Chem. Soc.* **1994**, *116*, 6220−6228.
(49) Ye, S.; Akutagawa, H.; Uosaki, K.; Sasaki, Y. *Inorg. Chem.* **1995**, *34*, 4527−4528.
(50) Van der Linden, J. G. M.; Heck, J.; Walther, B.; Bottcher, H. C. *Inorg. Chim. Acta* **1994**, *217*, 29−32.
(51) Blonk, H. L.; Mesman, J.; Van der Linden, J. G. M.; Steggerda, J. J.; Smits, J. M. M.; Beurskens, G.; Beurskens, P. T.; Tonon, C.; Jordanov, J. *Inorg. Chem.* **1992**, *31*, 962−968.
(52) Blonk, H. L. Thesis, University of Nijmegen, Nijmegen, The Netherlands, 1991; pp 1−115.
(53) Dupré, N.; Hendriks, H. M. J.; Jordanov, J.; Gaillard, J.; Auric, P. *Organometallics* **1984**, *3*, 800−802.
(54) Dupré, N.; Auric, P.; Hendriks, H. M. J.; Jordanov, J. *Inorg. Chem.* **1986**, *25*, 1391−1396.
(55) Mabbs, F. E.; Collison, D. *Electron Paramagnetic Resonance of Transition Metal Compounds*; Elsevier: Amsterdam, 1992.
(56) DeSimone, R. E. *J. Am. Chem. Soc.* **1973**, *95*, 6238−6244.
(57) Farmer, M. M.; Haltiwanger, R. C.; Kvietok, F.; Rakowski DuBois, M. *Organometallics* **1991**, *10*, 4066−4070.
(58) Kubas, G. J.; Ryan, R. R.; Kubat-Martin, K. A. *J. Am. Chem. Soc.* **1989**, *111*, 7823−7832.

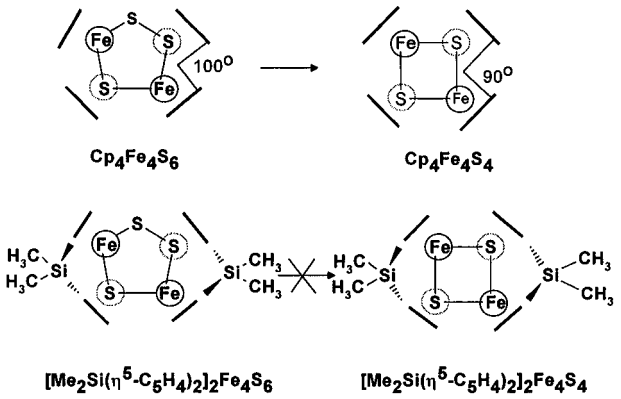

Figure 5. Schematic representation of the core contraction of Fe_4S_6 to Fe_4S_4. Solid circles represent Fe atoms in the front plane, and dashed circles, Fe atoms in the back plane.

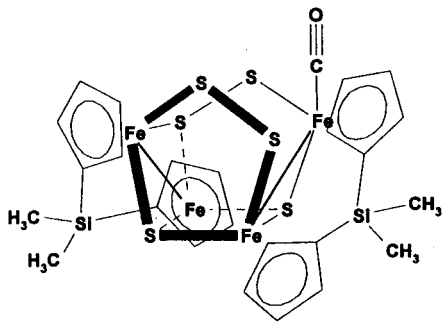

Figure 6. Proposed structure of $[Me_2Si(\eta^5\text{-}C_5H_4)_2]_2Fe_4S_6$ (CO) (**5**).

upon addition of Br_2 to **4**, the dication $\mathbf{4}^{2+}$ was obtained. According to its cyclic voltammogram, the resulting sample contained some impurities. After anion exchange with KPF_6, the product was still impure, but upon recording an ^1H NMR spectrum, we observed eight sharp cyclopentadienyl proton signals and two dimethylsilyl proton signals (Table 6). The C_5H_4 proton signals have clearly shifted downfield with respect to those of the neutral starting material. After crystallization of this PF_6 salt from acetone/diethyl ether in air, measurement of the equilibrium potential of an acetonitrile solution revealed that the compound had been reduced to the monocationic form [**4**]PF_6.

Conclusions. The introduction of silicon-bridged cyclopentadienyl ligands into iron−sulfur cluster chemistry provided a useful means for the preparation of new clusters, **3**−**5**. The flexibility in relative orientation of the two C_5H_4 rings of the $(\eta^5\text{-}C_5H_4)-SiMe_2-(\eta^5\text{-}C_5H_4)$ ligand is apparently limited for **4**. This prevents the expulsion of one or two sulfur atoms and the associated contraction of the iron−sulfur core previously observed for $Cp_4Fe_4S_6$ (see Figure 5).

The increased steric strain upon cluster-core contraction also seems to be indicated by the distinct positive shift of the potential of the second oxidation step of **4** as compared to $Cp_4Fe_4S_6$. However, other spectroscopic properties of **4** are very similar to those of $Cp_4Fe_4S_6$.

The reaction mechanism of the reaction of $[Me_2Si(\eta^5\text{-}C_5H_4)_2]Fe_2(CO)_4$ **(1)** with S_8 is complicated because iron is formally oxidized from +1 to +3 and sulfur is reduced from 0 to −2 (monosulfido groups), −1 (disulfido groups), or $-^1/_2$ (tetrasulfido group). Small sulfur catenane anions are known to form from S_8 upon electron uptake.[59−61] A part of the diiron starting complex has to be destroyed completely to generate the iron atoms for the central iron site in **3**. Notwithstanding this decomposition, the conversion of **1** to **3** and **4** is almost quantitative.

The photochemical reaction of $[Me_2Si(\eta^5\text{-}C_5H_4)_2]Fe_2(CO)_4$ **(1)** with S_8 yielded **5** as the only identifiable compound. Compound **5** may be considered as an intermediate in the thermal reaction, very close to the end of the reaction pathway (*in casu*, compound **4**). The proposed structure of **5** is shown in Figure 6. Compared to the case of **4**, the number of valence electrons at each iron center remains unchanged and an Fe−CO bond forms instead of an Fe−S bond. This would explain the ease of transformation of **5** into **4**.

Acknowledgment. We thank Mrs. A. Roelofsen (University of Nijmegen) for electrochemical measurements, Dr. F. Hartl (University of Amsterdam) for spectroelectrochemical measurements with the OTTLE cell,[6] Dr. F. Mulder (Kamerlingh Onnes Laboratory at Leiden University) and Dipl. Chem. S. Bieber (Hamburg University) for Mössbauer measurements, and Dipl. Chem. F. Moritz for EPR measurements. We are indebted to Prof. Dr. Ir. J. J. Steggerda for his continuing interest and fruitful discussions, and we are grateful for financial support from the SON/NWO.

Supporting Information Available: ^1H NMR spectra of **3**−**5**, Mössbauer spectra of **4** and [**4**]PF_6, cyclic voltammograms of **3**−**5**, IR spectra of **5** in various oxidation states, EPR spectra of frozen solutions of [**3**]PF_6 and [**4**]PF_6, and tables giving crystal data and structure refinement details, atomic coordinates and isotropic displacement parameters, bond lengths and angles, anisotropic displacement parameters, and hydrogen coordinates and isotropic displacement parameters (22 pages). Ordering information is given on any current masthead page.

IC960900+

(59) Paris, J.; Plichon, V. *Electrochim. Acta* **1981**, *26*, 1823−1829.
(60) Seel, F.; Güttler, H.-J.; Simon, G.; Wieckowski, A. *Pure Appl. Chem.* **1977**, *49*, 45−54.
(61) Bosser, G.; Paris, J. *New J. Chem.* **1995**, *19*, 391−399.
(62) Blonk, H. L.; Van der Linden, J. G. M.; Steggerda, J. J.; Jordanov, J. *Inorg. Chim. Acta* **1989**, *158*, 239−243.
(63) Jordanov, J.; Gaillard, J.; Prudon, M. K.; Van der Linden, J. G. M. *Inorg. Chem.* **1987**, *26*, 2202−2205.